Journal of Materials Chemistry A

Accepted Manuscript

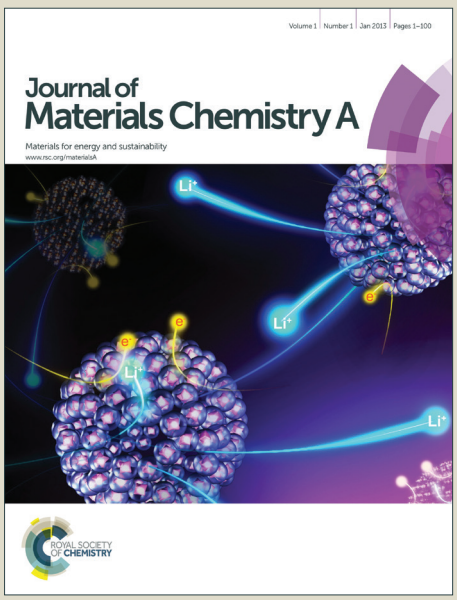

ROYAL SOCIETY OF CHEMISTRY

www.rsc.org/materialsA

Journal Name Journal of Materials Chemistry A Dynamic Article Links ►

Cite this: DOI: 10.1039/c0xx00000x

www.rsc.org/xxxxxx

ARTICLE TYPE

High Areal and Volumetric Capacity Sustainable All-Polymer Paper-Based Supercapacitors

Zhaohui Wang,* Petter Tammela, Peng Zhang, Maria Strømme,* Leif Nyholm*

Received (in XXX, XXX) Xth XXXXXXXXX 20XX, Accepted Xth XXXXXXXXX 20XX

DOI: 10.1039/b000000x

All-polymer paper-based electrodes with a thickness of up to hundreds of micrometers (e.g. 290 µm), large active mass loadings (> 20 mg cm^{-2}) and relatively high densities (1.23 g cm^{-3}) can be straightforwardly obtained from pristine low-cost polypyrrole-cellulose composites by decreasing the porosity of the material *via* space engineering. By straightforward compression of the composites, compact capacitive storage devices with improved space utilization are obtained without significantly compromising the electrochemical performance of the devices. This indicates that the compression unlike other methods previously used to vary the porosity of these composites does not affect the distribution of the mesopores which mainly determine the electrochemical performance of the material. When used to manufacture green supercapacitors comprising entirely of environmentally friendly materials, the freestanding and binder-free porous yet dense electrodes yield an areal capacitance of 5.66 F cm^{-2}, a device volumetric energy density of 3.7 Wh L^{-1} (based on the volume of the entire device) and the largest volumetric electrode capacitance of 236 F cm^{-3} so far reported for conducting polymer-based electrodes. The presented results for symmetric supercapacitors containing aqueous electrolytes represent significant progress in the development of inexpensive and environmentally friendly high-performance paper-based energy storage devices.

Introduction

Supercapacitors have recently attracted extensive attention due to their high power densities and their exceptional cycle life, although their energy densities normally are lower than those for lithium ion batteries.[1] Currently, significant research efforts are undertaken to develop high-performance supercapacitors with significantly improved energy densities.[2, 3] Despite the high reported gravimetric capacitances, many electrodes unfortunately fail to provide energy storage devices with high capacities due to the fact that the actual mass loadings of many electrodes and the apparent densities for the active materials are too low. [4, 5] In most cases the latter density was less than 0.75 g cm^{-3} which resulted in relatively low volumetric capacitances. With the mounting demand for compact and portable energy storage systems, there is growing interest to increase the utilization of the volume of the energy storage devices.[5, 6] Novel electrode materials with high volumetric capacitances and high mass loadings are consequently required to facilitate the manufacturing of inexpensive energy storage devices with improved volumetric energy densities and high capacities.

During the last few years, much work has been carried out to manufacture electrode materials with increased volumetric capacitances utilizing porous carbon-based materials including graphene,[5, 6] carbon nanotube-based composites[7-9], porous graphite oxide[10, 11] and porous carbon.[12, 13] While such materials can be charged and discharged fast and also exhibit large volumetric electrode capacitances (100 to 200 F cm^{-3} in most cases),[7, 10, 11, 13, 14] their typical active mass loading of ~ 1 mg cm^{-2} and electrode thicknesses of up to tens of micrometers are still significantly lower than those used in most commercially available electrochemical capacitors (i.e. 10 mg cm^{-2} , 100~200 µm),[4, 15] which results in energy storage devices with relatively low areal and volumetric capacities. It is therefore clear that additional research is required to ensure that the mass loading, bulk density (ρ) and the thickness of electrodes can be increased without significantly decreasing the electron and ion transport rates substantially.[5, 16] Other challenges are that many electrodes contain metals which can be relatively costly and that relatively high temperatures are used in the manufacturing processes which often require hours or even days. In addition, organic or corrosive aqueous electrolytes (e.g., KOH, H_2SO_4) with negative environmental impacts are often employed. The possibility of up-scaling the electrode materials with respect to economic and technical factors has also received very little attention in the literature so far. In the development of inexpensive, sustainable and safe energy storage devices with the capacities, shelf- and cycle lives required for commercial viability all the issues mentioned above consequently need to be addressed.[17, 18] This requires that new facile approaches for the fabrication of energy storage devices based on low-cost, compact and thick electrodes with large areal and volumetric capacitances are developed.

Recent advances in the development of conducting polymer and paper-based energy storage devices,[19-25] e.g. comprising PPy@nanocellulose electrodes consisting of polypyrrole (PPy) covered cellulose nanofibers,[26-30] open up new ways to address the challenges discussed above. It has thus been shown that conductive PPy-cellulose paper can be prepared within 30 minutes in aqueous solutions at room temperature using a straightforward and low-cost polymerization method.[19, 21] The resulting conductive all-polymer paper-based composites can directly be used as self-standing and binder-free electrodes with high mass loading (~10 mg cm^{-2}) in energy storage devices operating in aqueous NaCl solutions. This approach has also promising prospects in terms of environmental friendliness, simplicity, cost-efficiency and versatility; particularly as its up-scaling can benefit from existing industrial processes for paper making.[19] While the PPy@nanocellulose electrodes have been shown to exhibit specific capacitances of over 240 F g^{-1} PPy,[29] these as-formed electrodes, unfortunately, exhibit low packing densities (~0.4 g cm^{-3}) which yield low volumetric capacitances (< 100 F cm^{-3}). As this can be explained by the high porosity (i.e. up to 85%[29]) of the composites obtained as a result of the manufacturing process it is evident that there is a need for straightforward methods allowing the porosity to be decreased significantly while still maintaining sufficiently high mass transport rates to ensure that high power densities still can be obtained.

Herein, we show that thick all-polymer paper (APP) electrodes, with an active mass loading of up to 20 mg cm-2 and a thickness of 290 µm readily can be obtained merely by engineering the redundant space of the pristine *Cladophora* cellulose-PPy electrodes.[19, 26, 29] The latter yields a bulk density of up to 1.23 g cm^{-3} which is nearly twice the value commonly reported for activated porous carbon (i.e. 0.5 to 0.7 g cm^{-3}.[15]) We are not aware of any previous studies in which packing densities and electrode thicknesses as large as these have been described for a binder-less, free-standing composite electrode material. The thick, yet dense, free-standing APP electrodes exhibit volumetric capacitances of up to 236 F cm^{-3}, which are very high values for conducting polymer based electrodes, high areal capacitances of about 5.66 F cm^{-2} as well as a device energy density of 3.7 Wh L^{-1}. As the latter value, to the best of our knowledge, is the highest ever reported for a paper-based energy storage device, the presented results represent significant progress in the development of low-cost and environmentally friendly high-performance compact capacitive energy storage devices.

Experimental Section

Materials Synthesis

Cladophora green algae were collected from the Baltic Sea and the nanocellulose was extracted using grinding and acid hydrolysis as previously described.[31] Iron (III) chloride ($FeCl_3 \cdot 6H_2O$), hydrochloric acid (HCl), sodium chloride (NaCl), pyrrole and Tween-80 were purchased from Sigma-Aldrich and utilized as received. Deionised water was employed in all syntheses. The filter papers (Munktell, Sweden, General purpose filter papers, 20 µm thickness) used as the separators were used as obtained from Sigma-Aldrich.

Preparation of compact PPy@nanocellulose composites: *Cladophora* cellulose (300 mg) was dispersed in water (60 mL) by sonication using a total pulse time of 10 min and water cooling. The sonication was carried out using high-energy ultrasonic equipment (Sonics and Materials Inc., USA, Vibra-Cell 750) at an amplitude of 30% with a pulse length of 30 s and pulse-off duration of 30 s. Pyrrole (1 mL), Tween-80 (one drop) and 0.5 M HCl (40 mL) were mixed with the cellulose dispersion employing magnetic stirring for five minutes. PPy was then formed on the *Cladophora* cellulose fibres by chemical polymerization employing iron (III) chloride (8.65 g) dissolved in 0.5 M HCl (60 mL) as the oxidant. The polymerization was allowed to proceed for 30 min under stirring after which the composite was collected in an Büchner funnel connected to a suction flask and washed with 0.5 M HCl (5 L) followed by 0.1 M NaCl (0.5 L) to remove the remaining iron. The washed mixture was then drained on a polypropylene filter to form a filter cake, which was subsequently dried to form a paper sheet, in which the areal mass loading of PPy was ~ 20 mg cm^{-2}, if not stated otherwise. The PPy weight fraction in the composite has previously been shown to be about 67%.[26]

The as-prepared composite sheets (which typically had a thickness of 650 µm) were used to prepare compact APP electrodes by applying pressure. Two types of compressed samples were made using a compression force corresponding to one and five tons per cm^2, respectively, yielding thicknesses of the prepared composite sheets of 290 µm and 240 µm, respectively. The bulk density, i.e., the ratio between the mass of the sample and its volume, was estimated from the dimensions of a piece of composite, using a high precision digital calliper (Mitutoyo, Japan). The densities of the pristine, and the one and five ton compressed APP electrodes were 0.45, 1.02 and 1.23 g cm^{-3}, respectively. The corresponding porosities were estimated to be 74%, 38% and 26%, respectively.

Fabrication of symmetric supercapacitors: Symmetric devices, hermetically heat-sealed in a coffee-bag arrangement, were made as previously described.[26, 29] In these devices, the APP electrodes were directly used as electrodes without any addition of any polymeric binders or conductive additives. A piece of ordinary filter paper soaked with the 2 M NaCl electrolyte was used as the separator. The latter was sandwiched between two pieces of the composites (~1.0 cm × 1.0 cm) weighing between 29 and 32 mg, while graphite foils (with a thickness of 120 µm, SIGRAFLEX, SGL Carbon, Germany, grade Z) were used as current collectors.

Material and Electrochemical Characterizations

Scanning Electron Microscopy (SEM): SEM images for all samples were obtained employing a Leo Gemini 1550 FEG SEM instrument (Zeiss, Germany) operated at 1 kV employing an in-lens secondary electron detector. The samples were mounted on aluminium stubs with double-sided adhesive carbon tape and no sputtering was used prior to imaging.

Nitrogen sorption isotherm analysis: Nitrogen gas adsorption and desorption isotherms were measured with an ASAP 2020 instrument (Micromeritics, USA). The specific surface area was calculated according to the Brunauer-Emmett-Teller (BET) method[32] during adsorption and the pore size distribution was determined using the DFT method carried out with the DFT plus software from micrometrics using the model

for nitrogen adsorption at 77 K for slit-shape geometry with non-negative regularization and high smoothing (k = 0.02000).

Cyclic voltammetry: The cyclic voltammetry measurements were performed at room temperature employing an Autolab/GPES instrument (ECO Chemie, The Netherlands) with the synthesized APP electrode as the working electrode in a three-electrode electrochemical cell where a platinum wire served as the counter electrode and an Ag/AgCl electrode was used as the reference electrode. The composites used as the working electrode were cut out in the form of pieces weighing about 4 mg, which then were contacted by a platinum wire coiled around the sample. A solution of 2 M NaCl, purged with nitrogen for 10 min prior to the measurements, was used as the electrolyte. The voltammetry experiments were carried out at varying scan rates between 5 and 200 mV s^{-1}. In these experiments, the potential window was adjusted to compensate for the iR drop effect. (-0.8 ~ 0.6 V for scan rates from 5 to 50 mV s^{-1}; -0.8 ~ 0.8 V for scan rates 100 and 200 mV s^{-1}). The normalization of the cyclic voltammetric and charge capacity data was made with respect to the weight of APP electrode (containing about 67% of the active component, i.e. PPy).

Galvanostatic charge-discharge measurements: Galvanostatic charge-discharge measurements were carried out using a symmetric two-electrode set-up. Different current densities between 1 mA cm^{-2} and 200 mA cm^{-2} were then applied (a current density of 30 mA cm^{-2} was used in the cycling stability tests) as the cell was charged to a voltage of 0.8 V. During all measurements the cells were pressed with a clip applying a force of about 25 N to enable a good contact between the graphite sheet current collector and the APP electrodes.

Electrochemical Impedance Spectroscopy (EIS): EIS measurements were performed with a CH Instruments 660D potentiostat (CH Instruments, Inc., USA) at a cell potential of 0 V, using an ac amplitude of 10 mV. The frequency was varied between 100 kHz and 0.01 Hz.

Electrochemical data analysis

The specific gravimetric capacitance ($C_{electrode}$) and volumetric capacitance (C_{vol}) of one electrode were derived from the galvanostatic discharge curves using the following equations:

$$C_{electrode} = 4I\Delta t/(m\Delta V) \quad (1)$$

$$C_{vol} = \rho\, C_{\text{electrode}}, \quad (2)$$

where I denotes the discharge current and ΔV represents the potential change during the discharge time Δt, m is the total mass of both APP electrodes and ρ the density of the APP electrode. As the specific capacitances for symmetric supercapacitor devices often are calculated merely based on the active materials, the specific capacitances of the active materials, C_{wt}, were also calculated as:

$$C_{wt} = C_{electrode}/r_{electrode} \quad (3)$$

where $r_{electrode}$ denotes the PPy mass ration in one electrode.

The volume of the two electrodes as well as the volume of the entire device stack, including the two electrodes, the two current collectors (120 μm in thickness, each) and the one separator (20 μm in thickness) was used to calculate the volumetric energy densities $E_{vol\text{-}electrode}$ and $E_{vol\text{-}stack}$ for the electrodes and the devices, respectively. These were obtained as:

$$E_{vol\text{-}electrode} = C_{vol}\,(\Delta V)^2/8 \quad (4)$$

$$E_{vol\text{-}stack} = E_{vol\text{-}electrode} \cdot f_{electrode}, \quad (5)$$

where C_{vol} is the specific volumetric capacitance of one electrode, $E_{vol\text{-}electrode}$ denotes the volumetric energy density for <u>two</u> electrodes whereas $f_{electrode}$ represents the volumetric fraction of the two electrodes in a device.

The volumetric power density ($P_{vol\text{-}stack}$) normalized with respect to the volume of the device was calculated as:

$$P_{vol\text{-}stack} = E_{vol\text{-}stack}/\Delta t. \quad (6)$$

It is worth noting that several different metrics have been used to estimate capacitances as well as energy and power densities in the literature and that the data presented in the specific capacitance and Ragone plots in the literature often were calculated based on the mass of the active materials only. As was recently pointed out by Yang *et al.*[5] and Gogotsi and Simon,[4] such energy and power density values often represent overestimations leading to unrealistic claims, especially for electrode materials with low mass loadings and/or low packing densities. When comparing capacitance, energy and power density values reported in the literature, special caution hence needs to be taken to examine the metrics used in order to establish whether the electrode thickness and mass loadings were considered or not.

Results and Discussion

The *Cladophora* cellulose-PPy conductive composite materials, which were prepared within 30 min by chemical polymerization of pyrrole at room temperature, were directly used as binder-free electrodes, as is described in **Figure S1** in the Supporting Information (**SI**). The mass loading of the electrodes was 20 mg cm^{-2}, if not stated otherwise. As is seen in the inset of **Figure la** and the SEM images in **Figure 1a** and **b**, the obtained composite had the appearance of black glossy paper made up from numerous open, porous and loosely intertwined fibre structures, in good agreement with our previous results.[26, 33] To increase the density of the electrode material, the pristine material was compressed using a force corresponding to one or five tons per cm^2 which reduced the thickness of the material from 650 to 290 and 240 μm, respectively. As is seen in **Figure 1c** and **e**, the sample compressed using one ton per cm^2 exhibited a more compact structure and a rather flat surface. It is also seen that this material (in analogy with the pristine material) was composed of uniform intertwined PPy@nanocellulose fibres with an average diameter of about 90 nm as a result of the homogeneous coating of PPy on the *Cladophora* cellulose (see transmission electron microscopy (TEM) images in **Figure S2**, **SI**). The entangled nanofibers create three-dimensionally interfibre voids with pore sizes of tens of nanometres. For the sample exposed to the higher compression pressure corresponding to five tons per cm^2, the material exhibited a glossier and smoother surface but small voids distributed inside and between the PPy@nanocellulose fibres can still be observed throughout the material (see **Figure 1e** and **f**). This indicates that the material remained porous even after this compression. As is further demonstrated by the cross-section SEM images depicted in **Figure S3** (**SI**), the interconnected pore structure was also well maintained throughout the material.

Cite this: DOI: 10.1039/c0xx00000x

www.rsc.org/xxxxxx

ARTICLE TYPE

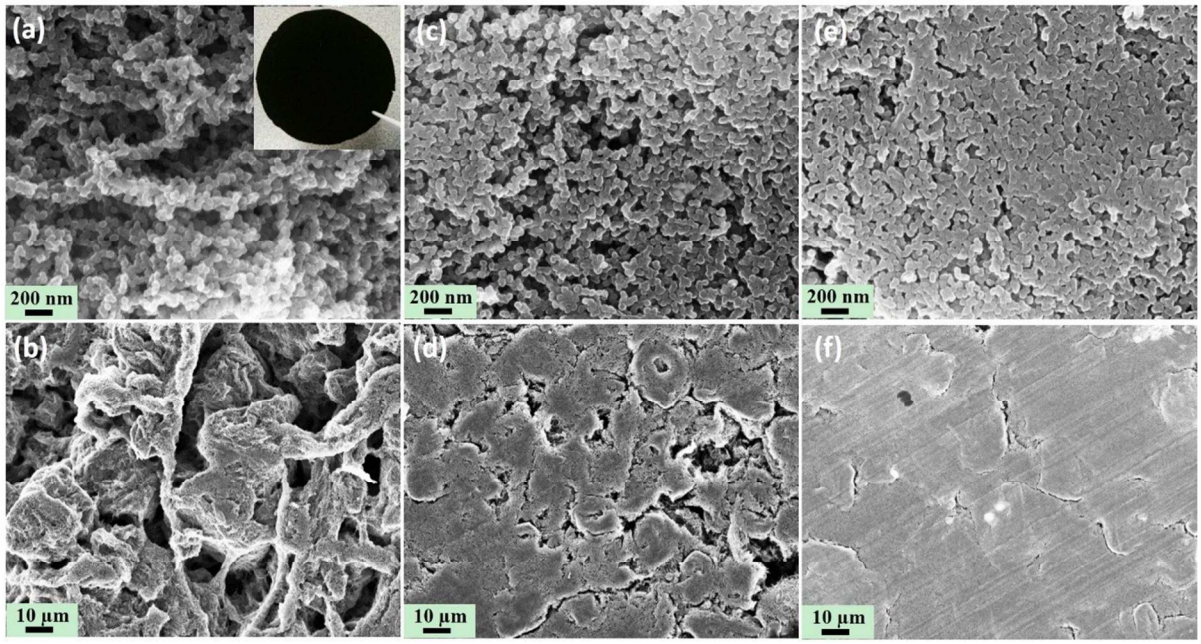

Figure 1. Low (a, c, e) and high (b, d, f) magnification SEM images of an uncompressed (i.e. pristine) APP electrode (a and b), APP electrodes obtained by applying a force corresponding to one ton per cm^2 (c and d) and five tons per cm^2 (e and f).

As shown in **Figure 2a**, N_2 sorption analysis indicated the presence of mesoporous microstructures for the uncompressed as well as compressed samples. The Brunauer-Emmett-Teller (BET) specific surface area (SSA) of the materials compressed using one and five tons per cm^2 were 39 and 36 m^2 g^{-1}, respectively, while that of the uncompressed sample was 53 m^2 g^{-1}. While these SSA values clearly are significantly smaller than those previously reported (> 500 m^2 g^{-1} in most case)[5, 6, 10, 11, 13] for dense carbon-based electrode materials, this does not hamper their electrochemical performance (as will be shown below) since the energy storage within the present material mainly involves oxidation and reduction of the PPy layer rather than charging of the double layer. In the present case it is hence sufficient to have a material which is porous enough to allow the PPy layer to be rapidly oxidized and reduced throughout the material. As this means that there should be a sufficiently high amount of electrolyte within the material the pore size distribution within the material is an essential parameter. To obtain a high volumetric energy density it thus is important to be able to remove the macropores which create unnecessary "dead electrolyte weight" while simultaneously maintaining the mesopores. The nitrogen sorption data analyzed in **Figure 2a** and **b** suggest that the observed decrease in SSA (**Figure 2a**) during compression mainly was due to the disappearance of macropores as only minor changes could be detected in the mesopore size distribution (**Figure 2b**). The latter is further supported by the SEM images (**Figure 1**). As a result of compression, the bulk density of the APP electrodes was increased from 0.45 g cm^{-3} for the pristine sample to 1.02 and 1.23 g cm^{-3} for the one and five ton compressed samples, respectively. The corresponding porosity of the samples was estimated to 74%, 38% and 26%, respectively. Since the present results suggest that the compacted materials have well-maintained mesoporous structures and the PPy layer on the cellulose fibres should give rise to a good surface wettability with respect to the aqueous electrolyte,[34] it can be expected that these compact materials should serve as APP electrodes with higher energy densities than their pristine counterparts as a result of the elimination of redundant pore volume (**Figure 2c**).

Cite this: DOI: 10.1039/c0xx00000x

www.rsc.org/xxxxxx

ARTICLE TYPE

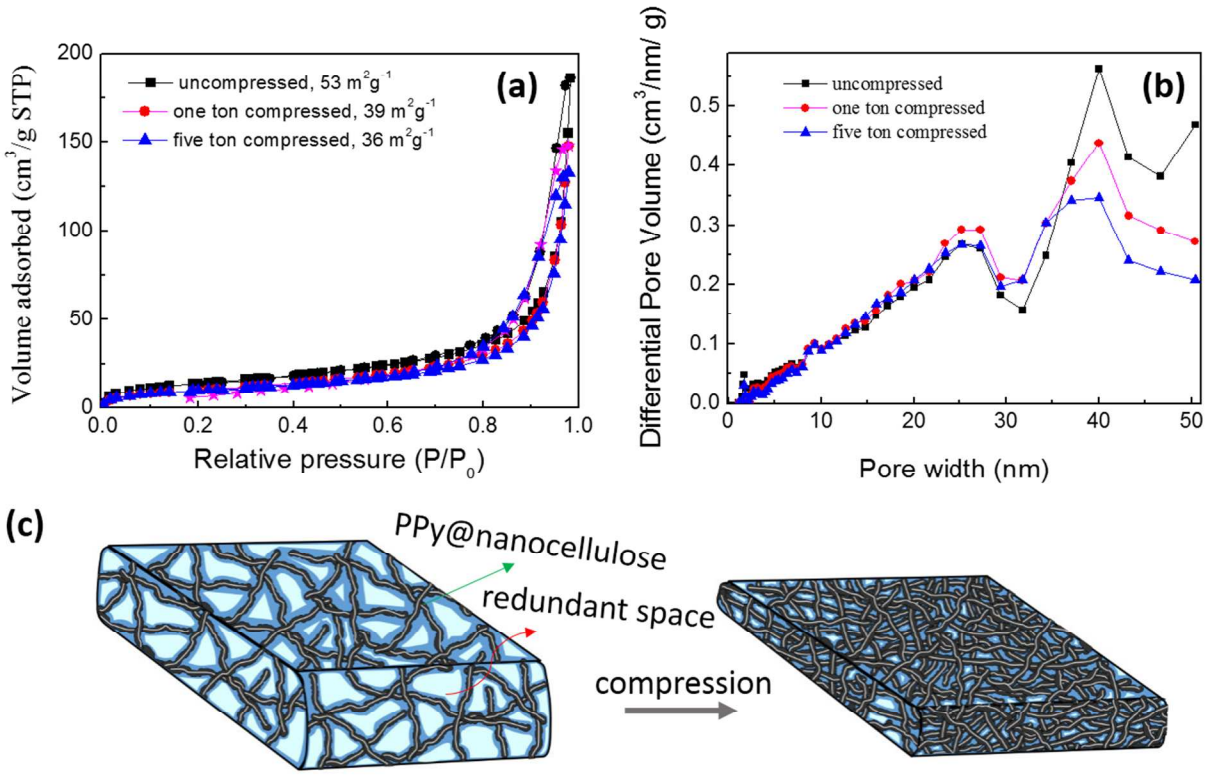

Figure 2 N_2 adsorption and desorption isotherms for uncompressed and compressed electrodes (a) and the corresponding pore size distributions (b). Schematic illustrations of the electrodes prior to (c, left) and after (c, right) compression in which brown fibres with black coating represent the PPy@nanocellulose fibres, the dark blue regions the mesopore regions close to the fibres and the light blue the macropores yielding the undesired "electrolyte dead weight".

To investigate the effect of density on the electrochemical performance of the APP electrodes, cyclic voltammograms (CVs) were recorded in an electrolyte composed of 2 M NaCl employing a three-electrode setup. As presented in **Figure 3a** and **b**, CVs with well-defined faradaic oxidation and reduction peaks were observed for all electrodes under study. More importantly and somewhat surprisingly, it can be seen that the CVs were practically identical for all samples. A very similar behaviour for all three electrodes was also seen when plotting the oxidation charge obtained from the CVs as a function of the scan rate for scan rates between 5 and 200 mV/s (see **Figure S4**, **SI)**. For the highest scan rate (i.e. 200 mV/s), the oxidation charge was still approximately 65% of that found for a scan rate of 5 mV/s for all three electrodes. These results indicate that the compression of the composite, which mainly removed the macropores present in the pristine composite, did not significantly influence the voltammetric performance of the composites. Since it is well-known that the pore size distribution within porous electrodes strongly affects the mass transport within such electrodes[35-37] it can be concluded that the electrochemical performance of the APP electrodes under study mainly is controlled by the mesopores. It has previously been shown[38, 39] that the porosity of PPy@nanocellulose composites can be tailored by employing different post-synthesis drying methods and that the electrochemical performance of these composites at scan rates up to 50 mV/s depended on the amount of electrolyte present within the porous electrode. When the porosity was decreased it was found that the ion mass transport was too slow to allow for full utilization of the inherent charge storage capacity for scan rates above 5 mV/s.[38] The good capacity retention at a scan rate of 50 mV/s observed for the compressed samples under study, however, suggests that the pore size distribution is more important than the porosity value as such. This is supported by the fact that the porosity of the most compressed sample in fact was lower than that of the samples used by Carlsson *et al.*[38, 39]. The latter is a very important finding as it implies that the energy density of the electrodes can be increased merely by compressing the electrodes whereas the previously employed approaches used to decrease the porosity appear to result in decreased capacities as a result of changes in the mesopore distribution. The latter may be explained by the fact that the polar environment surrounding the fibres during pressing in water effectively screens the charges on the surfaces of the fibres yielding a different fibre alignment

than that obtained when reducing the porosity with different drying approaches.

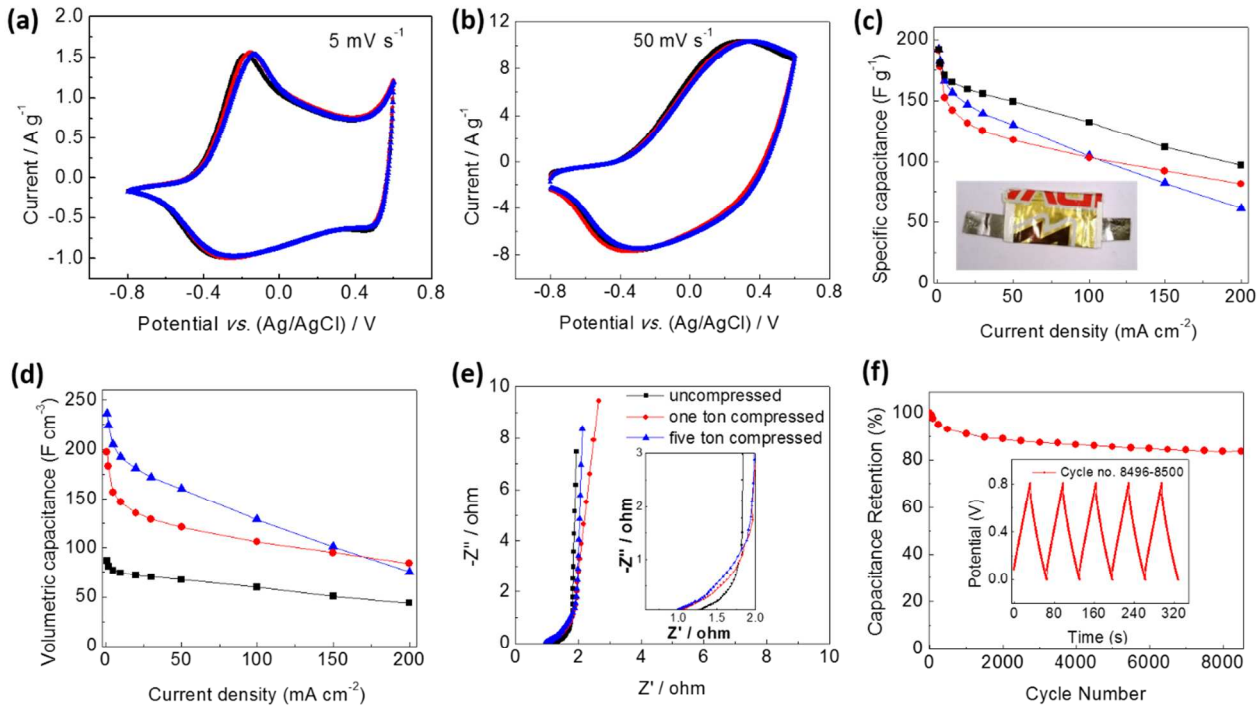

Figure 3 Electrochemical characterization of the uncompressed (ρ = 0.45 g cm^{-3}) and the two compressed composite electrodes (ρ = 1.02 and 1.23 g cm^{-3}, respectively) in 2.0 M NaCl based on cyclic voltammograms recorded at a scan rate of 5 mV s^{-1} (a) and 50 mV s^{-1} (b). Gravimetric (c) and volumetric (d) capacitances calculated based on constant current charge and discharge curves (see Figure S5, SI) using different charging/discharging current densities. (e) Nyquist plots (e) recorded using ac impedance measurements and (f) the cycling performance at 30 mA cm^{-2} for an APP electrode with a bulk density of 1.02 g cm^{-3}. The last five charge/discharge cycles are displayed in the inset. In all panels black, red and blue curves represent uncompressed, one ton per cm^2 and five ton per cm^2 compressed samples.

To further investigate the electrochemical performance of the composites, symmetric energy storage devices (see **Figure S1**, **SI)** were fabricated and subsequently tested in constant current charge/discharge experiments using a cell potential window between 0.0 and 0.8 V. The charge and discharge curves, which had the expected linear shapes (see **Figure S5**, **SI**) previously seen for this type of composites,[26, 29] indicated that the highest and lowest capacities at the highest current density were obtained for the pristine and the most compact electrodes, respectively. As the highest volumetric capacity at the lowest current density, on the other hand, was seen for the most compact sample it is evident that the decreased volume of the compressed samples only remains an advantage as long as the mass transport within the samples can keep up with the cycling rate. It should also be pointed out that the significant iR drop seen in the charge and discharge curves stems from the fact that a current density of up to 200 mA cm^{-2} (i.e. a current of up to 200 mA) was used in the experiments. While this current corresponds to about 10 A g^{-1} for the present mass loading, it would correspond to about 200 A g^{-1} for a mass loading of 1 mg cm^{-2} (typically used by many researchers). This point clearly demonstrates the problem with employing gravimetric current densities for samples with very different mass loadings and it can consequently be concluded that comparisons of energy storage devices should be carried out based on a number of parameters including the mass loadings of the electrodes. Since it is immediately evident that a larger mass loading will result in larger capacities and currents, larger iR drops will likewise be obtained as the capacity of the devices increases unless the cell resistance of the larger devices can be decreased simultaneously. As the present cell resistances of the present devices were of the order of 0.8 to 1.2 Ω, (values which incidentally most likely are significantly lower than for most previously reported devices) it is also clear that the cell resistance must be decreased significantly to enable the development of high capacity energy storage devices intended for use at high charge and discharge rates.[29]

A plot of the gravimetric specific electrode capacitance (obtained by multiplying the device capacitance by a factor of four) as a function of the current density (see **Figure 3c**) showed that same general behaviour as that seen in **Figure S5**. It can thus be seen that while the pristine sample demonstrated the highest capacitance at elevated current densities and that all three electrodes exhibited practically the same capacitance (i.e. ~190 F g^{-1} composite, corresponding to ~290 F g^{-1} PPy) for a current density of 1 mA cm^{-2}. This suggests that all of the PPy was electroactive at sufficiently low current densities for all three electrodes irrespectively of the density of the composite, in good agreement with previous findings.[38, 39] The absence of a significant difference between the three electrodes in the voltammetric experiments and the presence of such a difference in the chronopotentiometric experiments can be explained by the fact that the latter measurements are more sensitive to factors affecting the rate of the redox reactions (in the voltammetric

experiments there are no imposed demands on the rate of the reaction unlike in the controlled current case).

Table 1. A comparison of the performance of dense supercapacitor electrode materials.

Materials	ρ / g cm^{-3}	r / mg cm^{-2}	E_t / μm	C_{wt} / F g^{-1}	C_{ar} / mF cm^{-2}	C_{vol} / F cm^{-3}	Ref.
Commercial AC	0.5 ~ 0.7	~ 10	~ 200	160 ~ 200 *b*	N/A	80~110 *b*	15
CDC film	N/A	N/A	2, 100	N/A	N/A	160 *a*, 80 *a*	14
OMCNS	0.70	N/A	N/A	173 *a*	0.024	107 *a*	13
Compressed aMEGO	0.75	N/A	~ 60	147 *a*	N/A	110 *a*	10
A-aMEGO	1.15	~ 1	~ 90	154	~ 154	177	11
GO/CNTs	1.5	< 0.45	1 ~ 3	110 *a*	~ 50	165 *a*	7
EM-CCG films	1.25-1.33	1~10	< 80	197 ~ 209 *b*	~ 2000	231 ~ 261 *b*	5
rGO/PVP	0.4	N/A	1 ~ 4	179 *a*	31.6	71.8 *a*	40
rGO/PANI	0.76	N/A	N/A	210 *a*	N/A	160 *a*	41
PANI/Au/paper	N/A	0.47	N/A	560 *a* 40 *b*	300	N/A	24
PANI/Au/paper	N/A	2	10	400 *a* < 40 *b*	800	800 *a* ~ 80 *b*	24
rGO-PANI	0.57	N/A	~ 102	235 *b*	N/A	135 *b*	42
AAP	**1.02, 1.23**	**20**	**285** **240**	**288** *a* **192** *b*	**5660**	**354** *a* **236** *b*	**This work**

ρ : Bulk density; r : Mass loading; E_t : Electrode thickness; C_{wt} : Gravimetric capacitance; C_{ar} : Areal capacitance; C_{vol} : Volumetric capacitance. *a* : normalized with active mass; *b* : normalized with weight of electrode (active mass + conductive agent + binder);

Although it can be concluded that compression of the electrode gives rise to some loss of gravimetric capacitance (the most compressed composite exhibited a C_{wt} value of 61 F g^{-1} whereas the corresponding value for the pristine sample was 97 F g^{-1} at 200 mA cm^{-2}), the compression significantly increases the volumetric capacitance of the electrode (C_{vol}) at sufficiently low rates as is clearly seen in **Figure 3d**. In the latter figure it is likewise seen that C_{vol} for the most compressed sample remained higher than that of the pristine sample even at a current density of 200 mA cm^{-2} which corresponds to a charge time of less than four seconds. More importantly, as is seen **Table 1**, the C_{vol} value (i.e. 236 F cm^{-3}) exhibited by the most compressed composite sample at 1 mA cm^{-2} is, in fact, significantly higher than the values obtained for most compact porous carbon materials. In addition, the APP electrodes exhibited high areal capacitances of up to 5.66 F cm^{-2} which is much higher than those found for previous carbon-based and polymer-based supercapacitors electrodes (see **Table 1**). The present electrodes are also significantly thicker and hence have higher mass loadings than most other supercapacitor electrode materials. Given that the mass loading and thickness limit the capacity of the device and the fact that these parameters generally are difficult to scale up without loss of electrochemical performance as both C_{wt} and C_{vol} have been found to decrease with increasing thickness or mass loading of the electrodes,[5, 14, 16] the performance of the present APP electrodes is very promising. It should also be pointed out that the present mass loading (i.e. 20 mg cm^{-2}) and electrode thickness (i.e. 290 μm) represent values typically found in commercial devices.[15] One significant advantage of the material in present focus is that the mass loading (in mg cm^{-2}) may be varied merely by varying the thickness of the composite sheet. As very similar volumetric capacitances likewise were obtained for electrodes with an even larger mass loading of 36 mg cm^{-2}, (see **Figure S6**, **SI**), it is evident that the present APP electrodes can provide both high volumetric capacitances and high mass loadings. Electrodes with such properties are crucial for the realization of high-density electrochemical capacitive energy storage but have so far proved to be challenging to produce straightforwardly and inexpensively.[5]

Further studies of the symmetric energy storage devices were also performed using electrochemical impedance spectroscopy (EIS). As is seen in **Figure 3e**, a small equivalent series resistance of ~ 0.9 Ω was observed and the Nyquist plots also feature a nearly vertical curve in the low frequency range, indicating a typical (pseudo)capacitive behaviour. Such a performance is in good agreement with that expected for a device operating under thin-layer electrochemical conditions. The absence of a semicircle in the Nyquist plots further indicate that the electrochemical behaviour of the present electrodes is unaffected by electron transfer limitations in agreement with previous findings.[43] When going from low frequencies to higher frequencies, a diffusion-controlled region was seen as a line with a slope of about 45°, the extension of which increased slightly with an increase in the degree of compression of the composite

electrodes. A similar behaviour was likewise observed for graphene after employing a liquid-mediated dense integration process.[5] The EIS data in **Figure 3e** are hence in good agreement with the chronopotentiometric results as they show that the compression of the samples gives rise to a slightly increased influence of diffusion. The EIS results consequently confirm that the electrochemical performance remains practically the same even after compression of the samples and hence that the amount of electrolyte within the remaining mesopores is sufficient to ensure fast oxidation (and reduction) of the composite.

As is shown in **Figure 3f**, the long-time cycle performance of the symmetric energy storage devices was also investigated employing a current density of 30 mA cm^{-2} and a cell voltage window between 0.0 and 0.8 V. It is seen that about 84% of the initial capacitance remained after 8500 cycles for the compressed composite with a density of 1.02 g cm^{-3}, a performance which is comparable to or even better than for previously reported conducting polymer-based electrodes typically exhibiting 60~85% retention after 1000 cycles.[44] The rapid initial decrease in the capacitance (which often is seen for conducting polymer-based devices) could be related to the fact that the potential distribution between the two APP electrodes undergo significant changes during the initial part of the cycling which gives rise to some degradation of the positive electrode.[45] This is supported by the fact that the initial and final cycling curves generally have significantly different shapes (the insert in **Figure 3f** shows the last five charge and discharge curves for which the coulombic efficiency was very close to 100 %). No change in the morphology and structural properties with respect to that of the non-cycled material was observed after the long-time cycling experiment (see **Figure S7**, **SI**), in good agreement with our previous findings for the pristine composite.[45]

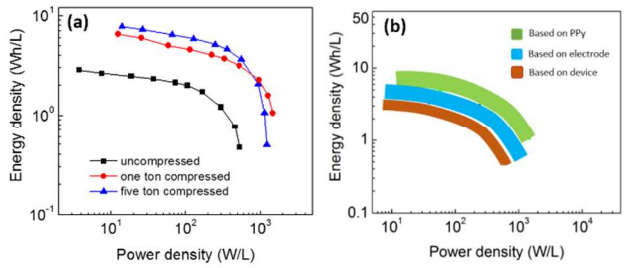

Figure 4 Ragone plots (a) for APP electrodes with different bulk densities and corresponding plots (b) for the compressed composite sample when calculated based on the volume of the PPy, the electrode and the device. The data were obtained from galvanostatic charge/discharge curves obtained in 2 M NaCl upon charging the device to 0.8 V.

The volumetric energy and power densities normalized with respect to the PPy, the electrode or the device volume were further calculated based on the results of the chronopotentiometric experiments in **Figure 3** (as is described in the experimental section). As shown in **Figure 4a**, the compression of the composite resulted in significant increases in both the volumetric energy and power densities of the electrodes. The electrode volumetric energy density ($E_{vol\text{-}electrode}$) was thus 5.2 Wh L^{-1} for the most compressed composite sample while the corresponding electrode volumetric power density was 980 W L^{-1}. These values are much higher than the corresponding values previously reported for carbon fibre reinforced PPy-based paper electrodes (i.e., 0.18 Wh L^{-1} and 270 W L^{-1})[29] and for graphite/PANI paper electrodes (i.e., 0.32 Wh L^{-1} and ~ 80 W L^{-1}).[46] In addition, **Figure 4b** compares the volumetric energy and power densities calculated based on the volumes of the active material, electrode and device, respectively. Since the electrodes contain about 67% of PPy, the volumetric energy and power densities are merely a factor of 1.5 larger than those calculated based on the volume of the active component (i.e. PPy). As this gives a volumetric energy density of 7.7 Wh L^{-1} for PPy, which is close to the theoretical volumetric energy density of 9.2 Wh L^{-1} for PPy, it is clear that the present electrodes are performing very well indeed. The latter theoretical value was calculated based on a theoretical capacity for PPy of 360 C g^{-1} (assuming a doping degree of 25% at +0.6 V vs. Ag/AgCl), yielding a theoretical energy density of 30 Wh kg^{-1} (PPy)[28] and the well-known assumption that the gravimetric values for a symmetric two-electrode device (normalized with the weight of both electrodes) should be four times lower than those obtained for a single electrode in a three-electrode experiments.[19] It should also be pointed out that the calculation above also assumes a symmetric potential distribution in the two-electrode cell and that the theoretical value will be lower if the potential distribution in the device is asymmetric.

As is seen in **Figure 4b**, the volumetric energy and power densities of the whole device was only a factor of 1.4 lower than the values calculated based on the volume of the electrode (or a factor of 2.1 lower than the values based on the volume of the active component, i.e. PPy). Since the volumetric energy and power densities of thin-film energy storage devices generally are 5 to 100 times lower than the values based on the volumes of the electrodes,[4] it is immediately clear that the performance of the present thick electrodes is very promising. The symmetric device containing two APP electrodes (both with a mass loading and thickness of 20 mg cm^{-2} and 240 µm, respectively) thus yielded a stack volumetric energy density ($E_{vol\text{-}stack}$) of 3.7 Wh L^{-1} which, to the best of our knowledge, is the highest value so far reported for paper and conducting polymer-based electrodes (see **Table S1**, **SI**). The latter value is in fact also close to those of many commercial carbon/carbon capacitors (5 ~ 8 Wh L^{-1})[15] operating with significantly higher cell voltages due to the use of organic electrolytes. It should, however, be mentioned that higher energy density values [22 Wh L^{-1};[47] 35 Wh L^{-1}[24]] have been reported for PANI hybrid electrodes composed of thin films of supported nanocomposites. As these values were normalized with respect to the very thin active layer, they cannot be compared with the values for the present electrodes with significantly higher mass loadings (and hence much larger total capacities). Since the present devices contain graphite current collectors which are six times thicker than the 20 µm thin current collectors normally used in the literature, it should also be possible to increase the $E_{vol\text{-}stack}$ value further to reach about 5.2 Wh L^{-1}. The present results consequently indicate that even though many parameters (such as the applied pressure, electrode thickness, potential window and the device fabrication process) not yet have been optimised, the all-polymer paper-based energy storage device can still be made to exhibit excellent electrochemical performance by merely tuning the packing density and controlling the pore size

distribution of the PPy and cellulose based composite electrodes.

Conclusions

We demonstrated that thick (e.g. 290 µm) and compact (1.23 g cm^{-3}) conductive PPy-nanocellulose paper-based all-polymer electrodes with excellent energy and power densities can be obtained through a straightforward compression of the composite electrodes. The latter process removes the macropores in the composite which are responsible for a large part of the dead weight and dead volume of the electrodes, while the mesopores, required for the attainment of excellent electrochemical performance, remain essentially unchanged. The dense, yet thick, PPy-nanocellulose paper electrodes therefore retain their porous structure providing the continuous ion transport network yielding very short charge and discharge times even for energy storage devices containing electrodes with mass loadings of up to 36 mg cm^{-2}. The present energy storage devices (which are composed entirely of environmentally friendly materials) exhibit areal capacitances of 5.66 F cm^{-2}, volumetric capacities of 236 F cm^{-3} (corresponding to 354 F cm^{-3} (PPy)) as well as a device volumetric energy densities of 3.7 Wh L^{-1}. As such a combination of values has been unattainable for conducting polymer-based electrodes previously, this holds great promise for the development of sustainable, cost-efficient, up-scalable and lightweight energy storage systems.

Notes and references

[a] *Department of Chemistry-The Ångström Laboratory, Uppsala University, Box 538, SE-751 21 Uppsala, Sweden, E-mail: zhaohui.wang@kemi.uu.se leif.nyholm@kemi.uu.se;*
[b] *Nanotechnology and Functional Materials, Department of Engineering Sciences, The Ångström Laboratory, Uppsala University, Box 534, SE-751 21 Uppsala, Sweden, E-mail: maria.stromme@angstrom.uu.se;*

† Electronic Supplementary Information (ESI) available: [details of any supplementary information available should be included here]. See DOI: 10.1039/b000000x/
‡ Footnotes should appear here. These might include comments relevant to but not central to the matter under discussion, limited experimental and spectral data, and crystallographic data.

1. R. Kötz and M. Carlen, *Electrochim. Acta*, 2000, **45**, 2483-2498.
2. P. Simon, Y. Gogotsi and B. Dunn, *Science*, 2014, **343**, 1210-1211.
3. G. Wang, L. Zhang and J. Zhang, *Chem. Soc. Rev.*, 2012, **41**, 797-828.
4. Y. Gogotsi and P. Simon, *Science*, 2011, **334**, 917-918.
5. X. Yang, C. Cheng, Y. Wang, L. Qiu and D. Li, *Science*, 2013, **341**, 534-537.
6. Y. Tao, X. Xie, W. Lv, D.-M. Tang, D. Kong, Z. Huang, H. Nishihara, T. Ishii, B. Li, D. Golberg, F. Kang, T. Kyotani and Q.-H. Yang, *Sci. Rep.*, 2013, **3**.
7. N. Jung, S. Kwon, D. Lee, D. M. Yoon, Y. M. Park, A. Benayad, J. Y. Choi and J. S. Park, *Adv. Mater.*, 2013, **25**, 6854-6858.
8. D. N. Futaba, K. Hata, T. Yamada, T. Hiraoka, Y. Hayamizu, Y. Kakudate, O. Tanaike, H. Hatori, M. Yumura and S. Iijima, *Nat. Mater*, 2006, **5**, 987-994.
9. H. R. Byon, B. M. Gallant, S. W. Lee and Y. Shao-Horn, *Adv. Funct. Mater.*, 2012, **23**, 1037-1045.
10. S. Murali, N. Quarles, L. L. Zhang, J. R. Potts, Z. Tan, Y. Lu, Y. Zhu and R. S. Ruoff, *Nano Energy*, 2013, **2**, 764-768.
11. M. Ghaffari, Y. Zhou, H. Xu, M. Lin, T. Y. Kim, R. S. Ruoff and Q. M. Zhang, *Adv. Mater.*, 2013, **25**, 4879-4885.
12. M. Heon, S. Lofland, J. Applegate, R. Nolte, E. Cortes, J. D. Hettinger, P.-L. Taberna, P. Simon, P. Huang, M. Brunet and Y. Gogotsi, *Energy Environ. Sci.*, 2011, **4**, 135-138.
13. X. Yu, J.-g. Wang, Z.-H. Huang, W. Shen and F. Kang, *Electrochem. Commun.*, 2013, **36**, 66-70.
14. J. Chmiola, C. Largeot, P.-L. Taberna, P. Simon and Y. Gogotsi, *Science*, 2010, **328**, 480-483.
15. A. Burke, *Electrochim. Acta*, 2007, **53**, 1083-1091.
16. J. Luo, H. D. Jang and J. Huang, *ACS Nano*, 2013, **7**, 1464-1471.
17. B. Dyatkin, V. Presser, M. Heon, M. R. Lukatskaya, M. Beidaghi and Y. Gogotsi, *ChemSusChem*, 2013, **6**, 2269–2280.
18. J. B. Goodenough, *Energy Environ. Sci.*, 2014, **7**, 14.
19. L. Nyholm, G. Nyström, A. Mihranyan and M. Strømme, *Adv. Mater.*, 2011, **23**, 3751-3769.
20. G. Zheng, Y. Cui, E. Karabulut, L. Wågberg, H. Zhu and L. Hu, *MRS Bull.*, 2013, **38**, 320-325.
21. L. Yuan, B. Yao, B. Hu, K. Huo, W. Chen and J. Zhou, *Energy Environ. Sci.*, 2013, **6**, 470-476.
22. I. Sultana, M. M. Rahman, J. Wang, C. Wang, G. G. Wallace and H.-K. Liu, *Electrochim. Acta*, 2012, **83**, 209-215.
23. Y. Yang, C. Wang, B. Yue, S. Gambhir, C. O. Too and G. G. Wallace, *Adv. Energy Mater.*, 2012, **2**, 266-272.
24. L. Yuan, X. Xiao, T. Ding, J. Zhong, X. Zhang, Y. Shen, B. Hu, Y. Huang, J. Zhou and Z. L. Wang, *Angew. Chem.*, 2012, **124**, 5018-5022.
25. D. Tobjörk and R. Österbacka, *Adv. Mater.*, 2011, **23**, 1935-1961.
26. G. Nystrom, A. Razaq, M. Stromme, L. Nyholm and A. Mihranyan, *Nano Lett.*, 2009, **9**, 3635-3639.
27. H. Olsson, D. O. Carlsson, G. Nyström, M. Sjödin, L. Nyholm and M. Strømme, *J.Mater. Sci.*, 2012, **47**, 5317-5325.
28. Z. Wang, P. Tammela, P. Zhang, M. Stromme and L. Nyholm, *J. Mater. Chem. A*, 2014, **2**, 7711-7716.
29. A. Razaq, L. Nyholm, M. Sjödin, M. Strømme and A. Mihranyan, *Adv. Energy Mater.*, 2012, **2**, 445-454.
30. L. Jabbour, R. Bongiovanni, D. Chaussy, C. Gerbaldi and D. Beneventi, *Cellulose*, 2013, **20**, 1523-1545.
31. A. Mihranyan, A. P. Llagostera, R. Karmhag, M. Strømme and R. Ek, *Intern. J. Pharm.*, 2004, **269**, 433-442.
32. S. Brunauer, P. H. Emmett and E. Teller, *J. Am. Chem. Soc.*, 1938, **60**, 309-319.
33. A. Mihranyan, L. Nyholm, A. E. G. Bennett and M. Strømme, *J. Phys. Chem. B*, 2008, **112**, 12249-12255.
34. Z. Wang, L. Qie, L. Yuan, W. Zhang, X. Hu and Y. Huang, *Carbon*, 2013, **55**, 328-334.
35. Z. S. Wu, Y. Sun, Y. Z. Tan, S. Yang, X. Feng and K. Mullen, *J. Am. Chem. Soc*, 2012, **134**, 19532-19535.
36. K. Xia, Q. Gao, J. Jiang and J. Hu, *Carbon*, 2008, **46**, 1718-1726.
37. C. Masarapu, L.-P. Wang, X. Li and B. Wei, *Adv. Energy Mater.*, 2012, **2**, 546-552.
38. D. O. Carlsson, A. Mihranyan, M. Strømme and L. Nyholm, *RSC Adv.*, 2014, **4**, 8489 – 8497.

39. D. O. Carlsson, G. Nyström, Q. Zhou, L. A. Berglund, L. Nyholm and M. Strømme, *J. Mater. Chem.*, 2012, **22**, 19014.
40. L. Huang, C. Li and G. Shi, *J. Mater. Chem. A*, 2014, **2**, 968-974.
41. Q. Wu, Y. Xu, Z. Yao, A. Liu and G. Shi, *ACS Nano*, 2010, **4**, 1963-1970.
42. D.-W. Wang, F. Li, J. Zhao, W. Ren, Z.-G. Chen, J. Tan, Z.-S. Wu, I. Gentle, G. Q. Lu and H.-M. Cheng, *ACS Nano*, 2009, **3**, 1745-1752.
43. G. Nyström, M. Strømme, M. Sjödin and L. Nyholm, *Electrochim. Acta*, 2012, **70**, 91-97.
44. G. A. Snook, P. Kao and A. S. Best, *J. Power Sources*, 2011, **196**, 1-12.
45. H. Olsson, G. Nyström, M. Strømme, M. Sjödin and L. Nyholm, *Electrochem. Commun.*, 2011, **13**, 869-871.
46. B. Yao, L. Yuan, X. Xiao, J. Zhang, Y. Qi, J. Zhou, J. Zhou, B. Hu and W. Chen, *Nano Energy*, 2013, **2**, 1071-1078.
47. J. Benson, I. Kovalenko, S. Boukhalfa, D. Lashmore, M. Sanghadasa and G. Yushin, *Adv. Mater.*, 2013, **25**, 6625-6632.

ToC figure

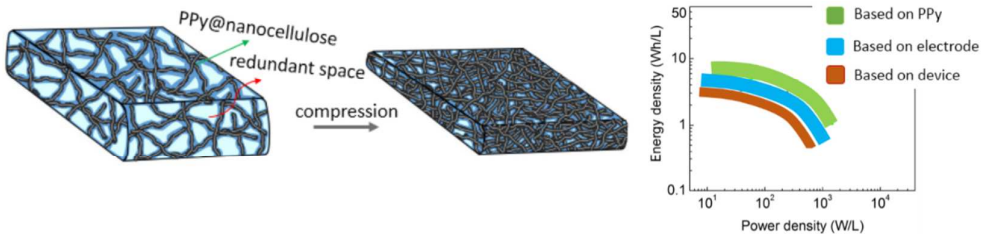

The table of contents

Dense, yet porous, all-polymer thick paper electrodes are constructed by straightforward compression of conducting PPy@nanocellulose composites. When used in symmetric supercapacitors, these electrodes yield a device volumetric energy density of 3.7 Wh L^{-1} as well as the highest volumetric specific capacitance (236 F cm^{-3}) and areal capacitance (5.66 F cm^{-2}) ever shown for paper and conducting polymer-based electrodes.